Progress In Electromagnetics Research, PIER 42, 233–246, 2003

ANALYSIS OF BI-ANISOTROPIC PBG STRUCTURE USING PLANE WAVE EXPANSION METHOD

L. G. Zheng and W. X. Zhang

State Key Laboratory of Millimeter Waves
Southeast University
No. 2, Si-Pai-Lou, Nanjing, Jiangsu, 210096, China

Abstract—An algebraic eigenvalue problem for analyzing the propagation characteristics of electromagnetic waves inside the PBG Structure consisting of complex medium is established by using Bloch theorem and plane wave expansion. Two eigen-solvers are employed. One is matrix-based and another is iterative. Calculated results show that both methods are effective for 2-D PBG structure, but the iterative eigen-solver is more attractive in both CPU-time and memory requirement. A sample of 2-D PBG structure, with Chiral medium as host and air cylinders arranged in triangular lattice as inclusion, is analyzed using both methods. It is found that the introduction of chirality increases the band gap width significantly.

1. INTRODUCTION

Many researched results on PBG structure have been published, since Yablonovitch [1–3] discovered that the propagation of EM waves into this structure is prohibited for a certain frequency band. On the analysis, the traditional method to analyze the multiple scattering of parallel cylinders using Hankel functions [34] requires great effort to deal with infinite periodical structure. The most popular methods are the PWE (Plane wave expansion method) [4–26] in frequency domain, FDTD [27] in time domain, and transfer matrix method [28–30] (a kind of mixed method). Among them PWE is more suitable for a structure with infinite periods, whereas FDTD is the best for a structure with finite periods. Besides, PWE is also one of the widely used method for analyzing 3-D PBG structure [4–9]. An open-source MIT Photonic-Bands Package [26] is a powerful tool for analyzing the PBG structure consisting of isotropic or anisotropic medium, based on the model of $\vec{H}$ wave equation derived from Maxwell equations. However, a PBG structure consisting of general complex medium, especially, bi-isotropic and bi-anisotropic material, had not been studied completely, and the dispersive are still unknown. The aim of this article is just to discover them by developing eigen value equations and then solving them using two effective eigen-solvers, one is matrix-based and the other is iterative.

2. LIST OF SYMBOLS USED

1. Primitive vectors of direct lattice in spatial space: $\vec{a}_1$, $\vec{a}_2$ and $\vec{a}_3$.
2. Direct lattice vectors in spatial space:
   $\vec{R} = n_1\vec{a}_1 + n_2\vec{a}_2 + n_3\vec{a}_3$, $\{n_i = 0, \pm1, \pm2, ... \pm N_i, i = 1, 2, 3\}$ are integers.
3. Primitive vectors of reciprocal lattice in spectral (wave number) space: $\vec{b}_1$, $\vec{b}_2$ and $\vec{b}_3$.
   $\vec{b}_1 = 2\pi\frac{\vec{a}_2\times\vec{a}_3}{V}$, $\vec{b}_2 = 2\pi\frac{\vec{a}_3\times\vec{a}_1}{V}$ and $\vec{b}_3 = 2\pi\frac{\vec{a}_1\times\vec{a}_2}{V}$, $V = \vec{a}_1 \cdot (\vec{a}_2 \times \vec{a}_3)$
4. Reciprocal lattice vectors in spectral space: $\vec{G} = m_1\vec{b}_1 + m_2\vec{b}_2 + m_3\vec{b}_3$, $\{m_i = 0, \pm1, \pm2, \pm3, ..., \pm M_i,\ i = 1, 2, 3\}$ are integers.
5. The definition of constitutive relations[31]:
   $$\begin{pmatrix} \vec{D} \\ \vec{B} \end{pmatrix} = \begin{pmatrix} \bar{\bar{\varepsilon}} & \bar{\bar{\xi}} \\ \bar{\bar{\zeta}} & \bar{\bar{\mu}} \end{pmatrix} \cdot \begin{pmatrix} \vec{E} \\ \vec{H} \end{pmatrix} \text{ or } \begin{pmatrix} \vec{E} \\ \vec{H} \end{pmatrix} = \begin{pmatrix} \bar{\bar{\kappa}} & \bar{\bar{\chi}} \\ \bar{\bar{\gamma}} & \bar{\bar{\nu}} \end{pmatrix} \cdot \begin{pmatrix} \vec{D} \\ \vec{B} \end{pmatrix}$$
6. Periodicity

Medium parameters are periodic with lattice vectors and can be written as:

$$\begin{pmatrix} \bar{\bar{\varepsilon}}(\vec{r}) & \bar{\bar{\xi}}(\vec{r}) \\ \bar{\bar{\zeta}}(\vec{r}) & \bar{\bar{\mu}}(\vec{r}) \end{pmatrix} = \begin{pmatrix} \bar{\bar{\varepsilon}}\left(\vec{r}+\vec{R}\right) & \bar{\bar{\xi}}\left(\vec{r}+\vec{R}\right) \\ \bar{\bar{\zeta}}\left(\vec{r}+\vec{R}\right) & \bar{\bar{\mu}}\left(\vec{r}+\vec{R}\right) \end{pmatrix}$$

$$\text{or} \begin{pmatrix} \bar{\bar{\kappa}}(\vec{r}) & \bar{\bar{\chi}}(\vec{r}) \\ \bar{\bar{\gamma}}(\vec{r}) & \bar{\bar{\nu}}(\vec{r}) \end{pmatrix} = \begin{pmatrix} \bar{\bar{\kappa}}\left(\vec{r}+\vec{R}\right) & \bar{\bar{\chi}}\left(\vec{r}+\vec{R}\right) \\ \bar{\bar{\gamma}}\left(\vec{r}+\vec{R}\right) & \bar{\bar{\nu}}\left(\vec{r}+\vec{R}\right) \end{pmatrix}$$

3. MATHEMATICAL MODAL

3.1. Wave Equation

In a source free, linear, inhomogeneous medium, Maxwell equations have the form

$$\begin{cases} \nabla \times \vec{E} = -j\omega\vec{B} \\ \nabla \times \vec{H} = j\omega\vec{D} \\ \nabla \cdot \vec{B} = 0 \\ \nabla \cdot \vec{D} = 0 \end{cases} \tag{1}$$

For isotropic and anisotropic media, the constitutional relations can be written as $\vec{D} = \varepsilon_0\bar{\bar{\varepsilon}} \cdot \vec{E}$, $\bar{\bar{\mu}} = \mu_0\bar{\bar{I}}, \bar{\bar{\xi}} = \bar{\bar{\zeta}} = \bar{\bar{0}}$, one can get wave equation about $\vec{H}$ from Eq. (1) as:

$$\nabla \times \left(\bar{\bar{\varepsilon}}\right)^{-1} \nabla \times \vec{H} = \frac{\omega^2}{c^2}\vec{H} \tag{2}$$

This is the widely used equation to analyze PBG material. A specific software, MPB [26] solves this eigenvalue H-equation using iterative method. When bi-anisotropic medium is involved, two of four fields ($\vec{E}, \vec{H}, \vec{D}$ and $\vec{B}$) must be used. Note that in Eq. (1), fields $\vec{D}$ and $\vec{B}$ are transverse everywhere while both $\vec{E}$ and $\vec{H}$ have no such property. Naturally it is more attractive to develop eigen equations containing only $\vec{D}$ and $\vec{B}$.

Eliminating $\vec{E}$ and $\vec{H}$ from Eq. (1) by using constitutive relations, we have

$$\nabla \times \begin{pmatrix} -\bar{\bar{\chi}} & -\bar{\bar{\kappa}} \\ \bar{\bar{\nu}} & \bar{\bar{\gamma}} \end{pmatrix} \cdot \begin{pmatrix} \vec{B} \\ \vec{D} \end{pmatrix} = j\omega \begin{pmatrix} \vec{B} \\ \vec{D} \end{pmatrix} \tag{3}$$

Or

$$\nabla \times [\mathbf{M}(\vec{r})] \cdot [\mathbf{F}(\vec{r})] = j\omega [\mathbf{F}(\vec{r})] \tag{4}$$

with notation of $[\mathbf{M}(\vec{r})] = \begin{pmatrix} -\bar{\bar{\chi}}(\vec{r}) & -\bar{\bar{\kappa}}(\vec{r}) \\ \bar{\bar{\nu}}(\vec{r}) & \bar{\bar{\gamma}}(\vec{r}) \end{pmatrix}$ and $[\mathbf{F}(\vec{r})] = \begin{pmatrix} \vec{B}(\vec{r}) \\ \vec{D}(\vec{r}) \end{pmatrix}$.

3.2. Eigenvalue Equations

According to Bloch theorem, the EM field in a periodic structure can be expressed as Bloch waves [32]:

$$[\mathbf{F}(\vec{r})] = e^{j\vec{k}\cdot\vec{r}}\,[\mathbf{f}(\vec{r})] \tag{5}$$

where $[\mathbf{f}(\vec{r})]$ is a periodic function with direct lattice $\vec{R}$ as its period: $\left[\mathbf{f}\left(\vec{r}+\vec{R}\right)\right] = [\mathbf{f}(\vec{r})]$ and $\vec{k}$ is a vector in the first Brillouin zone of wave number space. Writing $[\mathbf{f}(\vec{r})]$ in form of Fourier series, Eq. (5) becomes

$$[\mathbf{F}(\vec{r})] = e^{j\vec{k}\cdot\vec{r}}\,[\mathbf{f}(\vec{r})] = e^{j\vec{k}\cdot\vec{r}}\sum_{\vec{G}}\left[\mathbf{f}_{\vec{G}}\right]e^{j\vec{G}\cdot\vec{r}} = \sum_{\vec{G}}\left[\mathbf{f}_{\vec{G}}\right]e^{j(\vec{G}+\vec{k})\cdot\vec{r}} \tag{6}$$

where subscript $\vec{G}$ denotes quantum in Fourier space.

Those 6-element coefficients in Eq. (6) can be further reduced to 4-element ones using transversal characteristics of $\vec{D}$ and $\vec{B}$ fields. Substituting (6) into (1), one gets:

$$\nabla\cdot[\mathbf{F}(\vec{r})] = \sum_{\vec{G}} j(\vec{k}+\vec{G})\cdot\left[\mathbf{f}_{\vec{G}}\right]e^{j\left(\vec{k}+\vec{G}\right)\cdot\vec{r}} = [0] \tag{7}$$

Eq. (7) holds only when expressions $\left(\vec{k}+\vec{G}\right)\cdot\left[\mathbf{f}_{\vec{G}}\right] = [0]$ hold for each $\vec{G}$. In other words, for each $\vec{G}$, $\vec{B}_{\vec{G}}$ and $\vec{D}_{\vec{G}}$ lie in a plane with $\left(\vec{k}+\vec{G}\right)$ as its normal. Defining a $\vec{G}$-specific orthogonal coordinate system with unit vectors $\vec{e}_{1\vec{G}}$, $\vec{e}_{2\vec{G}}$ spanning the $\vec{B}_{\vec{G}} - \vec{D}_{\vec{G}}$ plane and $\vec{e}_{3\vec{G}} = \frac{(\vec{k}+\vec{G})}{|\vec{k}+\vec{G}|}$ as the third unit vector, we have

$$\begin{aligned}\left[\mathbf{f}_{\vec{G}}\right] &= \begin{pmatrix} \vec{B}_{\vec{G}} \\ \vec{D}_{\vec{G}} \end{pmatrix} = \begin{pmatrix} B_{1\vec{G}} \\ D_{1\vec{G}} \end{pmatrix}\vec{e}_{1\vec{G}} + \begin{pmatrix} B_{2\vec{G}} \\ D_{2\vec{G}} \end{pmatrix}\vec{e}_{2\vec{G}} \\ &= \begin{pmatrix} \vec{e}_{1\vec{G}} & \vec{e}_{2\vec{G}} & \vec{0} & \vec{0} \\ \vec{0} & \vec{0} & \vec{e}_{1\vec{G}} & \vec{e}_{2\vec{G}} \end{pmatrix}\begin{pmatrix} B_{1\vec{G}} \\ B_{2\vec{G}} \\ D_{1\vec{G}} \\ D_{2\vec{G}} \end{pmatrix}\end{aligned} \tag{8}$$

$$= \left[\mathbf{T}_{\vec{G}}\right]_{2\times 4}\left[\mathbf{f}_{\vec{G}}\right]_{4\times 1}$$

for each $\vec{G}$. Substituting (8) into (6) and then (6) into (3) yields:

$$\left(\nabla + j\vec{k}\right)\times\left[\mathbf{M}\left(\vec{r}\right)\right]\cdot\sum_{\vec{G}}\left[\mathbf{T}_{\vec{G}}\right]_{2\times 4}\left[\mathbf{f}_{\vec{G}}\right]_{4\times 1}e^{j\vec{G}\cdot\vec{r}} = j\omega\sum_{\vec{G}}\left[\mathbf{T}_{\vec{G}}\right]_{2\times 4}\left[\mathbf{f}_{\vec{G}}\right]_{4\times 1}e^{j\vec{G}\cdot\vec{r}} \tag{9}$$

Eq. (9) will be solved using both matrix-based eigensolver and iterative eigensolver.

3.3. Using Matrix-Based Eigensolver

3.3.1. Algebraic Eigenvalue Equations

In order to get explicit matrix, the media parameters must be further expressed in Fourier series as

$$\left[\mathbf{M}\left(\vec{r}\right)\right] = \sum_{\vec{G}}\left[\mathbf{M}_{\vec{G}}\right]e^{j\vec{G}\cdot\vec{r}},\ \left[\mathbf{M}_{\vec{G}}\right] = \int_{V}\left[\mathbf{M}\left(\vec{r}\right)\right]e^{-j\vec{G}\cdot\vec{r}}\,dV \tag{10}$$

where integral is done on a primitive cell formed by $\vec{a}_1$, $\vec{a}_2$ and $\vec{a}_3$.

Substituting Eq. (10) into (9) and using orthogonality of Fourier series, one gets

$$\sum_{\vec{G}'}\left\{\left[\mathbf{T}_{\vec{G}}\right]_{2\times 4}^{T}\cdot\left(\left(\vec{k}+\vec{G}\right)\times\left[\mathbf{M}_{\vec{G}-\vec{G}'}\right]\right)_{2\times 2}\cdot\left[\mathbf{T}_{\vec{G}'}\right]_{2\times 4}\right\}\cdot\left[\mathbf{f}_{\vec{G}'}\right]_{4\times 1} = \omega\left[\mathbf{f}_{\vec{G}}\right]_{4\times 1} \tag{11}$$

for all $\vec{G}$ in spectral space.

Eq. (11) is an algebraic eigen equations with a non-Hermitian matrix. It is ready to be solved by matrix-based eigensolvers such as ZGEEV in LAPACK from www.netlib.org.

3.3.2. Examples

The structure under consideration is an array of parallel air cylinders periodically arranged in triangular lattice in a Chiral medium. The dyadic medium parameters of a Chiral medium can be written as: $\bar{\bar{\varepsilon}} = \varepsilon_0\varepsilon_r\bar{\bar{I}}$, $\bar{\bar{\mu}} = \mu_0\mu_r\bar{\bar{I}}$, $\bar{\bar{\xi}} = (-j\kappa_r\sqrt{\varepsilon_0\mu_0})\bar{\bar{I}} = (-j\kappa_r c^{-1})\bar{\bar{I}}$ and $\bar{\bar{\zeta}} = -\bar{\bar{\xi}}$. Their values are: $\varepsilon_{hr} = 13$, $\mu_{hr} = 1$ for the host and $\varepsilon_{ir} = 1$, $\mu_{ir} = 1$, $\kappa_{ir} = 0$ for the inclusion. The geometrical parameters are: $|\vec{a}_1| = |\vec{a}_2| = a$, $r = 0.48a$.

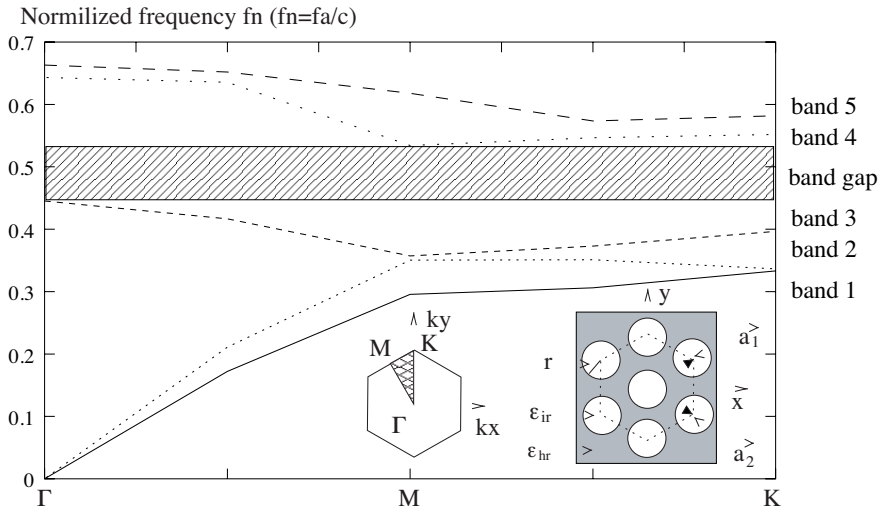

Figure 1. 2-D PBG structure and its dispersive curves. (An array of air cylinders(holes) arranged in triangular lattice in an isotropic host, $\varepsilon_{hr} = 13$, $\varepsilon_{ir} = 1$, $r = 0.48a$, $\kappa_{hr} = 0$).

(1) Band gap width at $\kappa_{hr} = 0$ (see Figure 1)

In this case, all the media are isotropic and both $\vec{D}\vec{B}$- and $\vec{H}$-equations can be used to calculate the band gap information and the results should be identical. In Table 1 only results from $\vec{H}$-equations are given. The band gap is located between band 3 and band 4. It is obvious that more expansion terms will lead to better accuracy. Hopefully the results based on $\vec{D}\vec{B}$-equations will follow the same rule but with different memory requirement: when $N = 35 \times 35 = 1225$, it requires an amount of $(1225 \times 4)^2 \times 32 \approx 768$ MBytes, which is more than we can afford. So the calculation of $\vec{D}\vec{B}$-equations is performed on a level of $N = 31 \times 31 = 961$, the memory requirement of which is about 476 MBytes. It will introduce a difference of 0.7% compared with result from MPB-code.

(2) Band gap width at different κ_{hr}

Table 2 lists the band gap width (between band 3 and band 4) behavior with respect to the relative host chirality κ_{hr}. We are confident at our results since the results at lower κ_{hr} are well meet with those from H-equation-based code. It can be found that the gap width is a function of the relative chirality of the host. The upper bound of κ_{hr} is $\kappa_{hr} \leq \sqrt{\varepsilon_{hr}\mu_{hr}} = 3.60555$ for lossless chiral medium [33].

Table 1. Band width convergence based on $\vec{H}$- equations (isotropic media).

Based on H-equation					
Using matrixed-eigensolver					From MPB-code
$N = N_1 \times N_2$	17×17	29×29	31×31	35×35	(iterative $\gg$ 35×35)
Gap width (%)	13.7	17.4	17.70	18.13	18.34

The potential maximal gap-width will be the double of the isotropic counterpart. The CPU time for one k-point is about 6 hours on a PC with Pentium IV 1.7 GHz CPU and 512 MB RAM.

Table 2. The band gap behavior with respect to the relative host chirality κ_{hr} ($N = 31 \times 31$).

Based on DB-equations										
κ_{hr}	1e-9	1e-5	0.1	1.0	2.0	2.5	2.75	3.0	3.3	3.6
Gap width(%)	17.70	17.70	17.73	21.13	29.95	35.36	35.98	35.33	30.97	19.43

3.4. Using Iterative Eigensolver

3.4.1. FFT

By examining Eq. (9) carefully, we can find out, from the point of view of functional concept, that, if using Dirac delta functions as test functions rather than the expansion functions themselves, one will get another set of algebraic equations. If the delta functions are set up at points in a primitive cell formed by $\vec{a}_1$, $\vec{a}_2$ and $\vec{a}_3$, i.e., $\vec{r}$ is limited in a primitive unit cell and can only locate in discrete point, then these $\vec{r}$'s can be written as:

$$\vec{r}_{n_1,n_2,n_3} = \frac{n_1}{N_1}\vec{a}_1 + \frac{n_2}{N_2}\vec{a}_2 + \frac{n_3}{N_3}\vec{a}_3 = \sum_{s=1}^{3} \frac{n_s}{N_s}\vec{a}_s, \quad n_s = 0, 1, 2, ..., N_s - 1 \tag{12}$$

Using orthogonality: $\vec{b}_p \cdot \vec{a}_s = \begin{cases} 2\pi & s = p \\ 0 & s \neq p \end{cases}$, $[\mathbf{f}(\vec{r}_{n_1,n_2,n_3})]$ in

Eq. (6) becomes

$$[\mathbf{f}(\vec{r}_{n_1,n_2,n_3})] = [\mathbf{f}_{n_1,n_2,n_3}] = \sum_{m_1,m_2,m_3} [\mathbf{f}_{m_1,m_2,m_3}] e^{j\sum_p \frac{2\pi m_p n_p}{N_p}} \tag{13}$$

where $\{m_i, i = 1, 2, 3\}$ comes from the vector decomposition of $\vec{G}$. Since both$[\mathbf{f}_{n_1,n_2,n_3}]$ and $[\mathbf{f}_{m_1,m_2,m_3}]$ consist of two 3-element vectors, Eq. (13) includes six discrete 3-D Fourier transforms. They can be computed effectively using FFT algorithm. The number of multiplying operations is $O(N \log_2 N)$, where N is the total grid points ($N = N_1 \times N_2 \times N_3$) (using $N_1 = M_1, N_2 = M_2, N_3 = M_3$ for unique solution).

3.4.2. One $\mathbf{Ax}$ *Operation for Iterative Eigensolver*

For iterative eigensolver, no matrix is explicitly established. In the process of iteration, the solver continuously provides column vectors and the user is responsible to create respective new column vectors based on $\mathbf{Ax}$ operation for problem $\mathbf{Ax} = \lambda\mathbf{x}$. From Eq. (9) one will figure out the steps one $\mathbf{Ax}$ operation will possess: inflate a 4N-element initial column vector into a 6N-element one; make FFT six times; multiply with media parameters at discrete point in primitive cell; make IFFT six times; finish curl operation on each spectral terms and deflate the 6N-element column vector into a 4N-element one. Note that in spatial space, the dot product of medium parameters with the field calculated from FFT at N points is a kind of diagonal matrix operation and the curl operation in wave number space is also a diagonal matrix operation. The FFT itself can be thought as a diagonal operation in point of view of the number of multiplication operation. This means that in one $\mathbf{Ax}$ operation, $\mathbf{x}$ operates on a sparse matrix $\mathbf{A}$. This is the main merit of iterative eigensolver.

Now Eq. (9) can be solved using iterative eigensolver like Implicitly Restarted Arnoldi Method(IRAM) in ARPACK which can also be found at web site: www.netlib.org.

3.4.3. Effective Medium Parameters

For matrix-based eigensolver, the accuracy of the calculated eigen values is only dominated by the number of the expansion terms. For iterative eigensolver, however, not only will the number of expansion terms play a role on accuracy, but the representation of media parameters at each field point as well. This happens especially near the interface of the two media. The simple treatment, that is, the values of the medium parameters come from the medium parameters at that

single field point, will lead to a different profile of the interface, a zigzagged one rather than a smooth one. When a point in a primitive unit cell is near the interface of two media, an effective rather than direct medium parameters should be used. In this way, the convergence of the iterative method as well as the accuracy of the eigen values can be improved. According to effective medium theorem, different polarized wave should be averaged in different way. Johnson [24] developed a way to compute effective medium for both isotropic and an-isotropic medium. We here develop a way to compute effective medium for bi-anisotropic medium.

(1) Splitting fields into normal and tangential components

$$\begin{aligned}\begin{pmatrix}\vec{D}\\ \vec{B}\end{pmatrix} &= \begin{pmatrix}\bar{\bar{\varepsilon}} & \bar{\bar{\xi}}\\ \bar{\bar{\zeta}} & \bar{\bar{\mu}}\end{pmatrix}\cdot\begin{pmatrix}\vec{E}\\ \vec{H}\end{pmatrix}\\ &= \left\{\begin{pmatrix}\bar{\bar{\varepsilon}} & \bar{\bar{\xi}}\\ \bar{\bar{\zeta}} & \bar{\bar{\mu}}\end{pmatrix}\cdot\begin{pmatrix}\vec{n}\vec{n} & 0\\ 0 & \vec{n}\vec{n}\end{pmatrix}+\begin{pmatrix}\bar{\bar{\varepsilon}} & \bar{\bar{\xi}}\\ \bar{\bar{\zeta}} & \bar{\bar{\mu}}\end{pmatrix}\cdot\begin{pmatrix}\vec{t}\vec{t} & 0\\ 0 & \vec{t}\vec{t}\end{pmatrix}\right\}\cdot\begin{pmatrix}\vec{E}\\ \vec{H}\end{pmatrix}\\ &= \begin{pmatrix}\vec{D}\\ \vec{B}\end{pmatrix}_{\vec{n}}+\begin{pmatrix}\vec{D}\\ \vec{B}\end{pmatrix}_{\vec{t}}\end{aligned}$$

where $\begin{pmatrix}\vec{D}\\ \vec{B}\end{pmatrix}_{\vec{n}} = \begin{pmatrix}\bar{\bar{\varepsilon}} & \bar{\bar{\xi}}\\ \bar{\bar{\zeta}} & \bar{\bar{\mu}}\end{pmatrix}\begin{pmatrix}\vec{n}\vec{n} & 0\\ 0 & \vec{n}\vec{n}\end{pmatrix}\begin{pmatrix}\vec{E}\\ \vec{H}\end{pmatrix}$, $\vec{t}\vec{t} = \bar{\bar{I}} - \vec{n}\vec{n}$, and $\begin{pmatrix}\vec{D}\\ \vec{B}\end{pmatrix}_{\vec{t}} = \begin{pmatrix}\bar{\bar{\varepsilon}} & \bar{\bar{\xi}}\\ \bar{\bar{\zeta}} & \bar{\bar{\mu}}\end{pmatrix}\begin{pmatrix}\vec{t}\vec{t} & 0\\ 0 & \vec{t}\vec{t}\end{pmatrix}\begin{pmatrix}\vec{E}\\ \vec{H}\end{pmatrix}$.

(2) Averaging medium in different way for different field components:

The underlying mechanism is very simple. Take $\vec{E}$ and $\vec{D}$ at the boundary of two isotropic media as an example. When crossing a dielectric boundary, the tangent component of $\vec{E}$ will be continuous and so is the normal component of $\vec{D}$. The averaged tangential component of $\vec{D}$ can be obtained from the product of the averaged permittivity and the common tangential component of $\vec{E}$. The averaged normal component of $\vec{E}$ can be obtained from the product of the averaged inverse of permittivity and the common normal component of $\vec{D}$. For boundaries involving bi-anisotropic media, the same rule applies.

$$\text{Ave}\begin{pmatrix}\bar{\bar{\varepsilon}} & \bar{\bar{\xi}}\\ \bar{\bar{\zeta}} & \bar{\bar{\mu}}\end{pmatrix}_{\vec{n}} = \left\{\frac{1}{V}\int_V\begin{pmatrix}\bar{\bar{\varepsilon}} & \bar{\bar{\xi}}\\ \bar{\bar{\zeta}} & \bar{\bar{\mu}}\end{pmatrix}^{-1}(\vec{r})\,dV\right\}^{-1}$$

$$\text{Ave}\begin{pmatrix} \bar{\bar{\varepsilon}} & \bar{\bar{\xi}} \\ \bar{\bar{\zeta}} & \bar{\bar{\mu}} \end{pmatrix}_{\vec{t}} = \frac{1}{V}\int_V \begin{pmatrix} \bar{\bar{\varepsilon}} & \bar{\bar{\xi}} \\ \bar{\bar{\zeta}} & \bar{\bar{\mu}} \end{pmatrix}(\vec{r})\, dV$$

where the integrals work on a small volume enclosing one single discrete grid point near the interface in a primitive cell formed by $\vec{a}_1$, $\vec{a}_2$ and $\vec{a}_3$. prefix "Ave" means "averaged"

(3)The total averaged medium:

$$\text{Ave}\begin{pmatrix} \bar{\bar{\varepsilon}} & \bar{\bar{\xi}} \\ \bar{\bar{\zeta}} & \bar{\bar{\mu}} \end{pmatrix} = \text{Ave}\begin{pmatrix} \bar{\bar{\varepsilon}} & \bar{\bar{\xi}} \\ \bar{\bar{\zeta}} & \bar{\bar{\mu}} \end{pmatrix}_{\vec{n}} \cdot \begin{pmatrix} \vec{n}\vec{n} & 0 \\ 0 & \vec{n}\vec{n} \end{pmatrix} + \text{Ave}\begin{pmatrix} \bar{\bar{\varepsilon}} & \bar{\bar{\xi}} \\ \bar{\bar{\zeta}} & \bar{\bar{\mu}} \end{pmatrix}_{\vec{t}} \cdot \begin{pmatrix} \vec{t}\vec{t} & 0 \\ 0 & \vec{t}\vec{t} \end{pmatrix}.$$

3.4.4. Examples

Before the convergence about the number of expansion terms is discussed, we'd like to know the influence of effective media. The parameters used are the same as in the example given in the section of matrix-based eigensolver. The number of expansion terms is a grid of 32×32, which is referred as the main grid. The averaging schemes are classified into four groups. Two of them are equal-space averaging on sub-grids of 32×32 and 64×64 respectively. The remaining two are calculated using 3- and 5-point Gaussian quadrature formulas.

(1) Comparison of frequency difference with respect to different averaging schemes.

Table 3 shows the maximum errors for different averaging scheme. The difference between 1024 (32×32) sampling points and 4096 (64×64) sampling points is very small whereas no averaging exhibits great errors. We use sub-grid 32×32 averaging scheme in further computation.

Table 3. Comparison of maximum frequency errors for different averaging scheme. Each error shown is the maximum one out of 24 frequencies (8 bands at 3 values of $\vec{k}$).

Averaging scheme	sub-grid		Gauss Formula		No Averaging
	32×32	64×64	3-point	5-point	
Maximum frequency error	0.00267%	0% (as reference)	0.827%	0.492%	2.785%

(2) Convergence behavior

Table 4 shows the influence of the number of expansion terms on frequency errors. At least 32×32 main grid size should be used in order to keep the errors small and the computation time acceptable.

Table 4. Comparison of maximum frequency errors for different numbers of expansion terms. Each error shown is the maximal one out of 24 frequencies (8 bands at 3 values of $\vec{k}$). The computation is done on a PC with Pentium IV 1.7 GHz CPU.

Main grid size	16×16	32×32	64×64	MPB-code
Maximum frequency error	2.597%	0.487%	0%(as reference)	1.244%
Band gap width	17.460%	18.842%	18.935%	18.343%
time consuming (one k-point)	$\sim$ 0.2minute	$\sim$ 2 minutes	$\sim$ 1 hour	$<$ 1 minute

(3) Band gap width with respect to different host chirality.

Table 5 shows the width of band gap for the same structure as Table 2. A difference of $35.98 - 32.64 = 3.34\%$ exists for gap width at $\kappa_{hr} = 2.75$ comparing width data in Table 5 and Table 2. This is not strange. The maximum frequency difference is much higher: 10.84%, but since the frequencies, which are used to calculating the width in Table 5 and Table 2, do not coincide with those maximum error frequencies, the width difference becomes smaller. When κ_{hr} is near 3.5, the matrix becomes singular and no results can be obtained.

Table 5. The band gap behavior with respect to the relative host chirality κ_{hr} (Main grid: 32×32; sub-grid: 32×32).

Based on DB equations and iterative eigensolver										
κ_{hr}	1e-9	1e-5	0.1	1.0	2.0	2.5	2.75	3.0	3.3	3.6
Gap width(%)	18.84	18.84	18.89	23.34	30.10	31.86	32.64	32.54	30.87	–

4. CONCLUSION

Eigen value equations are obtained using plane wave expansion method for photonic crystal consisting of bi-anisotropic media. The eigenvalue equations are solved using two different method: matrix-based method and iterative method. These two methods are all effective but behave differently. Iterative method seems to be more attractive in memory requirement and time consuming. When chiraliy is introduced, the width of band gap can be increased significantly.

REFERENCES

1. Yablonovitch, E., "Inhibited spontaneous emission in solid-state physics and electronics," *Phys. Rev. Lett.*, Vol. 58, No. 2, 2059–2062, 1987.
2. John, S., "Strong localization of photons in certain disordered dielectric superlattice," *Phys. Rev. Lett.*, Vol. 58, 2486, 1987.
3. Yablonovitch, E. and T. J. Gmitter, "Photonic band structure: The face-centered-cubic case," *Phys. Rev. Lett.*, Vol. 63, 1950, 1989.
4. Leung, K. M. and Y. F. Liu, "Full vector wave calculation of photonic band structures in face-centered-curbic dielectric media," *Phys. Rev. Lett.*, Vol. 65, No. 21, 2646–2649, 1990.
5. Satpathy, S. and Z. Zhang, "Theory of photon bands in three-dimensional periodic dielectric structures," *Phys. Rev. Lett.*, Vol. 64, No. 11 1239–1242, 1990.
6. Zhang, Z. and S. Satpathy, "Electromagnetic wave propagation in periodic structures: Bloch wave solution of Maxwell's equations," *Phys. Rev. Lett.*, Vol. 65 No. 21, 2650–2653, 1990.
7. Ho, K. M., C. T. Chan, and C. M. Soukoulis, "Existence of a photonic gap in periodic dielectric structures," *Phys. Rev. Lett.*, Vol. 65, No. 25, 3152–3155, 1990.
8. Sözüer, H. S. and J. W. Haus, "Photonic bands: Convergence problems with the plane-wave method," *Phys. Rev. B*, Vol. 45, No. 24, 13962–13972, June 15, 1992.
9. Kweon, G. and N. M. Lawandy, "Quantum electrodynamics in photonic crystals," *Optics Communications*, Vol. 118, 388–411, 1995.
10. Plihal, M., A. Shambrook, A. A. Maradudin, and P. Sheng, "Two-dimensional photonic band structures," *Opt. Commun.*, Vol. 80, No. 3,4, 199–204, 1991.
11. Plihal, M. and A. A. Maradudin, "Photonic band structure of two-dimensional systems: The triangular lattice," *Phys. Rev. B*, Vol. 44, No. 16, 8565–8571, 1991.
12. McCall, S. L., P. M. Platzman, R. Dalichaouch, D. Smith, and S. Schultz, "Microwave propagation in two-dimensional dielectric lattices," *Phys. Rev. Lett.*, Vol. 67, No. 15, 2017–2020, 1991.
13. Villeneuve, P. R. and M. Piché "Photonic band gaps in two-dimensional square and hexagonal lattices," *Phys. Rev. B, Condens. Matter*, Vol. 46, No. 8, 4969–4972, Aug. 1992.
14. Villeneuve, P. R. and M. Piché, "Photonic band gaps in two-

dimensional square lattices: Square and circular rods," *Phys. Rev. B, Condens. Matter*, Vol. 46, No. 8, 4973–4975, Aug. 1992.

15. Padjen, R., J. M. Gerard and J. Y. Marzin, "Analysis of the filling pattern dependence of the photonic bandgap for two-dimensional systems," *Journal of Modern Optics*, Vol. 41, No. 2, 295–310, 1994.
16. Maradudin, A. A. and A. R. McGurn, "Out of plane propagation of electromagnetic waves in a two-dimensional periodic dielectric medium," *Journal of Modern Optics*, Vol. 41, No. 2, 275–284, 1994.
17. Villeneuve, P. R. and M. Piché "Photonic band gaps of transverse-electric modes in two-dimensionally periodic media," *J. Opt. Soc. Am. A*, Vol. 8, No. 8, 1296–1305, 1991.
18. Anderson, C. M. and K. P. Giapis, "Larger two-dimensional photonic band gaps," *Phys. Rev. Lett.*, Vol. 77, No. 14, 2949–2952, 1996.
19. Qiu, M. and S. He, "Large complete band gap in two-dimensional photonic crystals with elliptic air holes," *Phys. Rev. B*, Vol. 60, No. 15, 10610–10612, 1999.
20. Li, Z.-Y., B.-Y. Gu, and G.-Z. Yang, "Large absolute band gap in 2D anisotropic photonic crystals," *Phys. Rev. Lett.*, Vol. 81, No. 12, 2574–2577, 1998.
21. Yang, H.-Y. D., "Surface-wave elimination in integrated circuit structures with artificial periodic materials," *Electromagnetics*, Vol. 20, 125–130, 2000.
22. Fan, S., P. R. Villeneuve, and J. D. Joannopoulos, "Large omnidirectional band gaps in metallodielectric photonic crystals," *Phys. Rev. B, Condens. Matter*, Vol. 54, No. 16, 11245–11251, Oct. 1996.
23. Meade, R. D., A. M. Rappe, K. D. Brommer, J. D. Joannopoulos, and O. L. Alerhand, "Accurate theoretical analysis of photonic band-gap materials," *Phys. Rev. B*, Vol. 48, 8434–8437, 1993. Erratum: S. G. Johnson, ibid Vol. 55, 15942, 1997.
24. Johnson, S. G. and J. D. Joannopoulos, "Block-iterative frequency-domain methods for Maxwell's equations in a planewave basis," *Optics Express*, Vol. 8, No. 3, 173–190, 2001.
25. Joannopoulos, J. D., R. D. Meade, and J. N. Winn, *Photonic Crystals: Molding the Flow of Light*, Princeton, 1995.
26. Johnson, S. G. and J. D. Joannopoulos, *The MIT Photonic-Bands Package*, http://ab-initio. mit.edu/mpb/.
27. Shumpert, J. D., W. J. Chappell, and L. P. B. Katehi, "Parallel-plate mode reduction in conductor-backed slots using

electromagnetic bandgap substrates," *IEEE Trans. on MTT*, Vol. 47, No. 11, 2099–2104, Nov. 1999.

28. Felbacq, D., G. Tayeb, and D. Maystre, "Scattering by a random set of parallel cylinders," *J. Opt. Soc. Am. A*, Vol. 11, No. 9, 2526–2538, Sept. 1994.
29. Bell, P. M., J. B. Pendry, L. M. Moreno, and A. J. Ward, "A program for calculating photonic band structures and transmission coefficients of complex structures," *Comput. Phys. Comm.*, Vol. 85, 306–322, 1995.
30. Pendry, J. B., "Photonic band structures," *Jour. of Modern Optics*, Vol. 41, No. 2, 209–229, 1994.
31. Kong, J. A., *Electromagnetic Wave Theory*, EMW Publishing, Cambridge, Massachusetts, USA, 2000.
32. Ashcroft, N. W. and N. D. Mermin, *Solid State Physics*, Chapter 8, Holt-saunders International Editions, 1976.
33. Lindell, I. V., *Advanced Field Theory*, 138 ss., tammikuu 2001.
34. Elsherbeni, A. Z., "Comparative study of two-dimensional multiple scattering techniques," *Radio Science*, Vol. 29, No. 4, Jul.–Aug. 1994.